RM A9J26

~~1109~~
~~190~~
c.2

NACA RM A9J26

4 APR 1950

NACA

RESEARCH MEMORANDUM

THE EFFECT OF ACCELERATING A HYPOTHETICAL AIRCRAFT THROUGH THE TRANSONIC RANGE WITH CONTROLS FIXED

By Howard F. Matthews

Ames Aeronautical Laboratory
Moffett Field, Calif.

NATIONAL ADVISORY COMMITTEE FOR AERONAUTICS
WASHINGTON
April 4, 1950

NATIONAL ADVISORY COMMITTEE FOR AERONAUTICS

RESEARCH MEMORANDUM

THE EFFECT OF ACCELERATING A HYPOTHETICAL AIRCRAFT THROUGH THE TRANSONIC RANGE WITH CONTROLS FIXED

By Howard F. Matthews

SUMMARY

Mach number histories of the motion experienced by a hypothetical, small, straight-wing aircraft accelerating at various rates through an assumed controls-fixed pitch-down balance change in the transonic range were obtained by a differential analyzer. For this particular case, the maximum change in normal acceleration is shown to increase with increasing longitudinal acceleration up to a certain magnitude of longitudinal acceleration, after which the maximum change in normal acceleration decreases with further increases in longitudinal acceleration. It is found that the Mach number variation of the angle of attack for static balance determines to a great extent the degree of the increase in the maximum change in normal acceleration. The effects of changes in attitude, altitude, moment of inertia in pitch, and a factor representative of the Mach number range of the balance change on the response of the aircraft are also noted.

Two approximate analytical solutions of the longitudinal equations of motion are developed which are based on certain simplifying assumptions indicated by the differential-analyzer results. Examples of each of these methods are presented and the results are shown to compare favorably with the differential-analyzer solutions. Computation time estimates for each method are also given.

INTRODUCTION

It is well known that conventional straight-wing aircraft experience unusual balance changes in the supercritical or transonic flight range. These balance changes may arise from a loss in lift at constant angle of attack, altered wing pitching-moment characteristics, a reduction of longitudinal-control effectiveness, or their combined effects. These are customarily summarized in reports by a plot of horizontal stabilizer incidence or elevator angle for steady level flight as a function of Mach number. The rapid and sometimes rather large changes in longitudinal control deflection necessary for balance shown on such plots, which are usually accompanied by changes in control force for balance, led to the belief that a pilot may have difficulty maintaining steady level flight as the aircraft accelerates through the transonic range. In addition, he possibly may apply adverse control deflection due to his relatively slow reaction time and inability to transmit changes in attitude or normal acceleration into proper corrective control deflection, especially since the effectiveness of the control may be rapidly varying. For these reasons, the proposal of accelerating through this region with fixed longitudinal control was advanced, with the further supposition that increasing the longitudinal acceleration might reduce considerably the effect of the attendant balance changes on the motion of the aircraft. It may be mentioned that the foregoing also has its correlative problem in the accelerating phase of the flight of supersonic guided missiles, including those launched from high subsonic speed aircraft.

A brief study was made, therefore, of the effect of longitudinal acceleration on the normal acceleration, particularly the maximum normal acceleration, for a hypothetical straight-wing aircraft subjected to an assumed pitch-down balance change in the transonic range. Due to the complexity imposed by the assumed nonlinear variation of the aerodynamic parameters with Mach number, a differential analyzer was used to permit rapid simultaneous solution of the three longitudinal equations of motion.

To make possible the solving of these equations of motion without the use of specialized computational equipment, simplified approximate analytical procedures were developed based on the results from the differential analyzer. These approximate analytical methods also lead to an indication of the effect of longitudinal acceleration on the estimation of steady-state stability characteristics obtained by the research technique of programmed control motions of rocket-powered models.

NOTATION

A_l longitudinal acceleration factor, the ratio of the net aerodynamic force in the direction of the relative wind (positive when directed forward) to the weight of the airplane $\left(\frac{a\dot{M}}{g}\right)$

A_n normal acceleration factor, the ratio of the net aerodynamic force perpendicular to the relative wind (positive when directed upward) to the weight of the airplane $\left(\frac{C_L}{C_{L_{trim}}}\right)$

C_D drag coefficient $\left(\frac{\text{drag}}{qS}\right)$

C_L lift coefficient $\left(\frac{\text{lift}}{qS}\right)$

$C_{L_{trim}}$ airplane lift coefficient for steady level flight $\left(\frac{W}{qS}\right)$

C_{L_α} lift-curve slope of complete airplane

$C_{L_{\alpha_t}}$ lift-curve slope of the horizontal tail

C_m pitching-moment coefficient about the center of gravity $\left(\frac{\text{pitching moment}}{qS\bar{c}}\right)$

C_{m_o} pitching-moment coefficient about the center of gravity for zero i_t, δ_e, and C_L

$C_{m_{C_L}}$ static longitudinal stability parameter $\left(\frac{\partial C_m}{\partial C_L}\right)$

$C_{m_{i_t}}$ stabilizer effectiveness parameter $\left(\frac{\partial C_m}{\partial i_t}\right)$

$C_{m_{\delta_e}}$ elevator effectiveness parameter $\left(\frac{\partial C_m}{\partial \delta_e}\right)$

I_Y pitching moment of inertia, slug-feet squared

M Mach number $\left(\frac{V}{a}\right)$

S wing area, square feet

S_t horizontal-tail area, square feet

T thrust, pounds

V velocity, feet per second

W weight of aircraft, pounds

a velocity of sound, feet per second

b wing span, feet

c wing section chord, feet

$\bar{c}$ wing mean aerodynamic chord $\left(\frac{\int_0^{b/2} c^2 dy}{\int_0^{b/2} c\ dy}\right)$, feet

g	gravitational acceleration, feet per second squared
h_p	pressure altitude, feet
i_t	stabilizer angle
l_t	tail length, feet
m	mass of aircraft $\left(\frac{W}{g}\right)$, slugs
n_t	tail efficiency factor $\left(\frac{q_t}{q}\right)$
q	free-stream dynamic pressure $\left(\frac{1}{2}\rho V^2\right)$, pounds per square foot
q_t	dynamic pressure at the horizontal tail, pounds per square foot
t	time, seconds
y	lateral coordinate of wing section chord, feet
α	angle of attack
α_o	angle of attack for zero lift
γ	flight-path angle $(\theta-\alpha)$
δ_e	elevator angle
ϵ	angle of downwash at the horizontal tail
ζ	ratio of damping of the complete airplane to that of the horizontal tail
θ	angle of pitch
ρ	mass density of air, slugs per cubic foot

All angles are in radians unless otherwise noted. A dot $(\cdot)$ or double dot $(\cdot\cdot)$ above a symbol represents, respectively, the first and second derivative with respect to time. The subscripts i and s refer to initial and static-balanced conditions, respectively. The term "static balanced" is used herein to specify the values of α, C_L, or A_n, which give zero pitching moment in steady (no longitudinal acceleration) flight.

DIFFERENTIAL-ANALYZER CALCULATIONS FOR HYPOTHETICAL AIRCRAFT

Method of Analysis

Since in the transonic speed range the aerodynamic parameters which influence the motion of an airplane are generally nonlinear functions of Mach number, the simultaneous solution of the longitudinal equations of motion appeared too time consuming for a normal step-by-step procedure. Therefore, the differential analyzer at the University of California at Los Angeles was used to solve these equations of motion.

A number of solutions were obtained corresponding to different variations of the important aerodynamic parameters with Mach number; changes in initial altitude and attitude, and several magnitudes of constant thrust. This was done with a twofold purpose: first, to show the mechanics of the motion of an airplane subjected to a balance change in the transonic range, particularly with regard to the maximum change in A_n developed, for different constant thrusts (or, as examination of results later showed, approximately constant longitudinal acceleration A_l for thrust values of practical interest); and, second, to provide information relative to a possible simplification of the longitudinal equations of motion or other artifice leading to an analytical solution.

It was realized that in the transonic range the aerodynamic parameters are not only nonlinear functions of Mach number, but also of angle of attack at high lift coefficients. This nonlinearity in angle of attack would have offered no difficulty in solving the equations of motion on the differential analyzer, but it was neglected partly because it was felt to be of secondary importance and partly due to the belief that it could not be taken into account in any practical or simple analytical approach.

For each solution, the airplane was assumed initially to be in steady flight at a stated altitude, attitude, and a Mach number of 0.90. A given constant thrust was then applied to accelerate the airplane through the transonic range.

Equations of Motion

If damping in pitch and the lag in downwash at the tail are the only nonstatic aerodynamic effects considered, the equations of longitudinal motion in wind-axis notation are:

$$T \cos \alpha - q\, S\, C_D - W \sin \gamma = m\dot{V}$$

$$-T \sin \alpha - q\, S\, C_L + W \cos \gamma = -m\, V\, \dot{\gamma}$$

$$q\, S\bar{c}\, C_m - \frac{qS_t l_t^2}{V}\, n_t\, C_{L_{\alpha_t}} \left(\zeta\dot{\theta} + \frac{d\epsilon}{d\alpha}\, \dot{\alpha} \right) = I_Y\, \ddot{\theta}$$

where C_L is assumed equal to $C_{L_\alpha}(\alpha-\alpha_o)$ and C_m equal to C_{m_o} + $C_{m_{i_t}} i_t + C_{m_{\delta_e}} \delta_e + C_{m_{C_L}} C_L$.

The physical limitations of the differential analyzer made necessary the assumption that the mass, moment of inertia, and thrust remained constant with time. An additional simplification was to consider the cosine of the angle of attack equal to unity and the sine equal to the angle in radians.

Assumed Characteristics of Hypothetical Airplane

The geometric and mass characteristics assumed are:

S, square feet	150
S_t, square feet	30
$\bar{c}$, feet	5
l_t, feet	12.5
W, pounds	7,500
I_Y, slug-feet squared	10,000 (unless otherwise noted)

The variation of aerodynamic parameters with Mach number is shown in figure 1. Three variations with Mach number are given in this figure for the lift-curve slope and the angle of attack for zero lift. The applicable variation is denoted in subsequent figures by the letters a, b, or c. Initial level flight at a pressure altitude of 50,000 feet was used unless otherwise indicated. The ratio of the damping of the complete airplane to that of the tail ζ was assumed to be constant and equal to 1.15, and the tail efficiency factor n_t equal to 1.0.

Results and Discussion

Since the terms "static-balanced angle of attack" and "static-balanced normal acceleration" occur frequently in the subsequent discussion, it is believed desirable to clarify by two examples the definition given in the section Notation. For instance, if tail damping is negligible, the static-balanced condition can be thought of as a steady turn of a radius of curvature just sufficient to develop the static-balanced normal acceleration A_{n_s} and static-balanced angle of attack α_s at the particular Mach number under consideration. Likewise, the lift coefficient and angle of attack assumed by a free-floating model with the pivot point at the assumed center of gravity are representative of static-balanced conditions.

Usually the response of an airplane to a disturbance is illustrated by a time history of appropriate quantities. For this particular study, however, it is believed more meaningful to plot the response as a Mach number history, since the basic balance change or forcing function, represented by α_s or A_{n_s}, is independent of longitudinal acceleration when plotted as a function of Mach number.

As may be seen from the equations of motion, the instantaneous values of the aerodynamic loads and associated moments have been assumed to be completely defined by the angle of attack of the lifting surface; that is, the lag in the build-up of circulation due to unsteady motions has been neglected. It follows that any dynamic effect of longitudinal acceleration must arise through its influence upon the pitching response of the aircraft. For the pitch-down balance change defined by characteristics (a) of figure 1, figure 2 shows that the dynamic effect of longitudinal acceleration occurs as an increasing initial speedwise lag in angle of pitch with increasing longitudinal acceleration.

In figure 2 and most of the succeeding figures, the average longitudinal acceleration $A_{l_{av}}$ corresponding to each value of constant thrust is noted. The longitudinal acceleration was found to be nearly constant over the Mach number range at high values of thrust, but increasing deviations from a constant magnitude occurred at lower thrusts. It is partly for this reason that data at low thrusts are omitted and partly due to the fact that the extreme changes in attitude and altitude and the relatively large time interval necessary to traverse the balance change associated with low thrusts preclude their practicability.

In figure 3 are plotted Mach number histories of the angle of attack and normal acceleration for the same average longitudinal accelerations as in figure 2 and for the static-balanced condition. It is apparent from this figure that at a relatively low value of $A_{l_{av}}$ the response of the aircraft follows closely the static-balanced condition with increasing departures occurring at higher accelerations. At some magnitude of $A_{l_{av}}$, a peak in the maximum change of normal acceleration is reached, which, for the conditions assumed, is appreciably greater percentagewise than for a low value of $A_{l_{av}}$, although the actual magnitude of the increase in g is small due to the extreme altitude. This effect of longitudinal acceleration upon the maximum change in normal acceleration (or to the ratio of the maximum change in dynamic to static-balanced normal acceleration, which, for convenience, will be referred to hereafter as the normal-acceleration response ratio) is largely dependent upon the variation of the static-balanced angle of attack with Mach number. Figure 4 shows the results of a number of solutions by the differential analyzer for three variations of α_s but an identical variation of A_{n_s} with Mach number. The variations in α_s were obtained by changing the

Mach number variation of α_o and C_{L_α}. It is seen that the most pronounced effect of longitudinal acceleration upon normal acceleration occurs for the condition of the greatest variation of α_s with Mach number.

Comparatively large changes in initial flight-path angle (0° and 30°), moment of inertia (5,000, 10,000, and 20,000 slug-ft^2), and altitude (30,000, 40,000, and 50,000 ft) have relatively little effect on the magnitude of the peak of the normal-acceleration response ratio. A change in Mach number width of the balance change, the width being defined herein as the Mach number increment between the initial Mach number and that for maximum change in A_{n_s}, also has little effect on the peak normal-acceleration response ratio if A_{n_s} and α_s plotted as a function of percent of the Mach number width of the balance change remain the same. As illustrated in figure 5, independent changes in moment of inertia, Mach number balance change width, and altitude have an appreciable effect on the magnitude of the average longitudinal acceleration at which the peak normal-acceleration response ratio occurs. The assumed balance change in this instance is of a larger magnitude than that for previous figures, but it is believed that the results in figure 5 indicate the general trend.

From the data presented, it is apparent that, if the Mach number width of the balance change is of the order of 0.05, the total thrust capabilities of transonic research aircraft may place them in a region where the normal acceleration is appreciably affected by longitudinal acceleration.

SIMPLIFIED COMPUTATION METHODS

Since a differential analyzer is not always available, the development of relatively quick approximate analytical methods by which the response of an aircraft to longitudinal acceleration could be computed was believed desirable. In the following two methods, the validity of the assumptions made in developing these methods was indicated by the results from the differential analyzer and was substantiated in each case by comparing the normal acceleration computed by the analytical method with the differential-analyzer answers for two values of longitudinal acceleration. These methods are based on reducing the three longitudinal equations of motion to a single differential equation in angle of attack which is of the second order, linear, and nonhomogeneous.

Modified Step by Step

Theory.- Examination of Mach number histories for the longitudinal accelerations considered revealed that the flight-path angle (but not $\dot{\gamma}$)

was relatively constant. Since the time interval to traverse the balance change is small, resulting in little change in altitude, the density of the air and speed of sound also can be considered unchanged during the flight.

If V is replaced by aM and $\dot{V}$ by $a\dot{M}$, the two force equations may be combined by eliminating thrust and the longitudinal equations reduce to the following:

$$\dot{\alpha} = \dot{\theta} - \left[\left(\frac{1}{2}\frac{\rho a S}{m}\right)_K M\left(C_{L_\alpha} + C_D\right) + \left(\dot{M} + \frac{g}{a}\sin\gamma_i\right)_K \frac{1}{M}\right]\alpha +$$

$$\left(\frac{1}{2}\frac{\rho a S}{m}\right)_K M C_{L_\alpha}\alpha_o + \left(\frac{g}{a}\cos\gamma_i\right)_K \frac{1}{M} \qquad (1)$$

$$\ddot{\theta} = \left(\frac{1}{2}\frac{\rho a^2 S\bar{c}}{I_Y}\right)_K M^2\left[C_{m_o} + C_{m_{i_t}} i_t + C_{m_{\delta_e}}\delta_e + C_{m_\alpha}(\alpha - \alpha_o)\right] -$$

$$\left(\frac{1}{2}\frac{\rho a S_t l_t^2}{I_Y}\right)_K M n_t C_{L_{\alpha_t}}\left(\zeta\dot{\theta} + \frac{d\epsilon}{d\alpha}\dot{\alpha}\right) \qquad (2)$$

where the terms enclosed with parenthesis with a subscript K are constant. Differentiation of equation (1) gives

$$\ddot{\alpha} = \ddot{\theta} - \left[\left(\frac{1}{2}\frac{\rho a S}{m}\right)_K M\left(C_{L_\alpha} + C_D\right) + \left(\dot{M} + \frac{g}{a}\sin\gamma_i\right)_K \frac{1}{M}\right]\dot{\alpha} -$$

$$\left[\left(\frac{1}{2}\frac{\rho a S}{m}\right)_K \overline{M(C_{L_\alpha} + C_D)}^{\,\bullet} + \left(\dot{M} + \frac{g}{a}\sin\gamma_i\right)_K \left(\dot{\frac{1}{M}}\right)\right]\alpha +$$

$$\left(\frac{1}{2}\frac{\rho a S}{m}\right)_K \overline{M C_{L_\alpha}\alpha_o}^{\,\bullet} + \left(\frac{g}{a}\cos\gamma_i\right)_K \left(\dot{\frac{1}{M}}\right) \qquad (3)$$

It is advantageous to evaluate the term $\left(\dot{\frac{1}{M}}\right)$ at this time.

$$\frac{d(1/M)}{dt} = -\frac{\dot{M}}{M^2} \tag{4}$$

Substituting equations (1), (2), and (4) into equation (3) to eliminate θ and its derivatives and noting that

$$-C_{m_\alpha}\alpha_s = C_{m_o} + C_{m_{i_t}} i_t + C_{m_{\delta_e}}\delta_e - C_{m_\alpha}\alpha_o$$

the equations of motion reduce to the following single, second-order, linear, nonhomogeneous differential equation with variable coefficients:

$$\ddot{\alpha} + b\dot{\alpha} + k\alpha = f \tag{5}$$

where

$$b = \left(\frac{1}{2}\frac{\rho a S}{m}\right)_K M\,(C_{L_\alpha} + C_D) + \left(\dot{M} + \frac{g}{a}\sin\gamma_i\right)_K \frac{1}{M} +$$

$$\left(\frac{1}{2}\frac{\rho a S_t l_t^2}{I_Y}\right)_K M\,n_t\,C_{L_{\alpha_t}}\left(\zeta + \frac{d\epsilon}{d\alpha}\right)$$

$$k = -\left(\frac{1}{2}\frac{\rho a^2 S\bar{c}}{I_Y}\right)_K M^2 C_{m_\alpha} + \left(\frac{1}{2}\frac{\rho a S_t l_t^2}{I_Y}\right)_K M\,n_t\,C_{L_{\alpha_t}}\,\zeta\Bigg[\left(\frac{1}{2}\frac{\rho a S}{m}\right)_K M\,(C_{L_\alpha} + C_D) +$$

$$\left(\dot{M} + \frac{g}{a}\sin\gamma_i\right)_K \frac{1}{M}\Bigg] + \left(\frac{1}{2}\frac{\rho a S}{m}\dot{M}\right)_K \frac{d[M(C_{L_\alpha} + C_D)]}{dM} -$$

$$\frac{\left(\dot{M}^2 + \frac{g}{a}\dot{M}\sin\gamma_i\right)_K}{M^2}$$

$$f = -\left(\frac{1}{2}\frac{\rho a^2 S\bar{c}}{I_Y}\right)_K M^2 C_{m_\alpha}\alpha_s + \left(\frac{1}{2}\frac{\rho a S_t l_t^2}{I_Y}\right)_K M\, n_t\, C_{L_{\alpha_t}}\zeta\left[\left(\frac{1}{2}\frac{\rho a S}{m}\right)_K M\, C_{L_\alpha}\alpha_o + \right.$$

$$\left.\left(\frac{g}{a}\cos\gamma_i\right)_K \frac{1}{M}\right] + \left(\frac{1}{2}\frac{\rho a S}{m}\dot{M}\right)_K \frac{d(M\, C_{L_\alpha}\alpha_o)}{dM} - \frac{\left(\frac{g}{a}\dot{M}\cos\gamma_i\right)_K}{M^2}$$

Equation (5) is recognizable as the fundamental equation of simple, damped, vibratory motion with the exception that in this instance the coefficients b and k, representative of the damping and the spring constant, respectively, are nonlinear functions of Mach number or time. Therefore, consider the case in which the Mach number range under investigation is divided into a number of intervals, the interval being chosen sufficiently small so that the variables b and k can be assumed constant in magnitude and f a linear function of Mach number. The solution of equation (5) for constant coefficients can take any one of three forms, depending on whether both roots of the auxiliary equation are real and unequal $(b/2)^2 > k$, real and equal $(b/2)^2 = k$, or complex $k > (b/2)^2$ and can be found in any standard text on differential equations or vibrations. The following is the solution (in terms of M since $t = \Delta M/\dot{M}$) for the most common case of $k > (b/2)^2$:

$$\alpha = e^{\frac{-b}{2\dot{M}}\Delta M}\left[A\cos\left(\frac{\sqrt{k-(b/2)^2}}{\dot{M}}\Delta M\right) + B\sin\left(\frac{\sqrt{k-(b/2)^2}}{\dot{M}}\Delta M\right)\right] +$$

$$F_0 + \frac{F_1}{\dot{M}}\Delta M \tag{6}$$

$$\dot{\alpha} = e^{\frac{-b}{2\dot{M}}\Delta M}\left[\left(B\sqrt{k-(b/2)^2} - (b/2)A\right)\cos\left(\frac{\sqrt{k-(b/2)^2}}{\dot{M}}\Delta M\right) - \right.$$

$$\left.\left(A\sqrt{k-(b/2)^2} + (b/2)B\right)\sin\left(\frac{\sqrt{k-(b/2)^2}}{\dot{M}}\Delta M\right)\right] + F_1 \tag{7}$$

where

f is represented by $f_{\Delta M=0} + \frac{df}{dM} \Delta M$

$$F_1 = \left(\frac{df}{dM} \frac{\dot{M}}{k} \right)$$

$$F_0 = \frac{f_{\Delta M=0} - bF_1}{k}$$

$$A = \alpha_{\Delta M=0} - F_0$$

$$B = \frac{\dot{\alpha}_{\Delta M=0} + (b/2)\, A - F_1}{\sqrt{k - (b/2)^2}}$$

The Mach number interval is denoted by ΔM and the initial $\dot{\alpha}_{\Delta M=0}$ is obtained from equation (1) by assuming $\dot{\theta}$ equal to zero. The Mach number history of angle of attack of the aircraft is computed step by step by means of equations (6) and (7) for each Mach number interval, the initial conditions of one interval being equal to the end boundary conditions of the previous interval. The motion of the airplane can then be completely defined by obtaining the angle of pitch from equation (1).

Results and discussion.— The necessary curve fitting and computations of an example are shown in figure 6 and table I, respectively. The selection of ΔM (a constant value of 0.02 for the example shown) is obviously an important factor and is a compromise between the ΔM for minimum computation time and the ΔM for greatest accuracy. The optimum value is clearly that magnitude which will give the desired accuracy in the minimum time and may be best selected by the examination of the computations at a number of values of ΔM. The ΔM need not be the same for each interval, but the computations are reduced slightly if it is constant. The results of this example and one at a higher value of $A_{l_{av}}$ are compared with the differential-analyzer answers in figure 7. It is evident that by this method good correlation is obtained with the differential-analyzer Mach number histories.

Initially, it may appear that this method is at least as time consuming as the normal step-by-step procedure, but a careful scrutiny of the equations defining b, k, and f shows that only portions of these factors are affected by $\dot{M}$, and then only in a simple manner. This is a very important time-saving characteristic if Mach number histories are desired for a number of longitudinal accelerations. Some simplification in the factors b, k, and f usually may be made. For instance, C_D is normally negligible compared to C_{L_α} even in the transonic region, and the portion of k containing the tail damping may be negligible, depending upon the amount of static stability. It has been estimated that, given the necessary aerodynamic data in the form as shown in figure 1, a Mach number history in angle of attack for one longitudinal acceleration would require approximately two and a half computer days and that each succeeding longitudinal acceleration would necessitate about one additional computer day.

A study of the terms forming the coefficients b, k, and f of equation (5) indicates that there are two basically different effects of longitudinal acceleration; one that arises from the terms which are functions of $\dot{M}$; and the other from the fact that different longitudinal accelerations cause the assumed disturbance to be traversed in different lengths of time or periods. The latter effect is analogous to that of first-order vibrating system in which the amplitude of the response depends both on the magnitude of the input disturbance and on the ratio of its frequency to the natural frequency of the system. For simple disturbances then, an estimation of the longitudinal acceleration for maximum change in normal acceleration may be made by computing the $\dot{M}$ which will result in the period of the disturbance being equal to the average natural period of the airplane.

A method of research in the transonic range which is being increasingly utilized is the rocket-powered model flight, wherein the controls are programmed to have simple motions throughout the flight and the response of the model measured by appropriate instruments. Much useful information is obtained from these tests, such as an estimation of the static and dynamic-stability characteristics derived from the period and damping of the oscillation following the control deflection. The period and time to damp are inversely proportional to the coefficients $\sqrt{k-(b/2)^2}$ and b, respectively, of equation (5). It appears from an examination of these coefficients that appreciable errors can occur in the determination of the stability of the full-size configuration from the powered portion of such flights of high longitudinal accelerations are developed during this period and for this reason the coasting portion of flight is used for the data analysis.

Equivalent-Disturbance Method

<u>Theory</u>.- The differential-analyzer results indicated that the Mach number history of A_{n_s} (or C_{L_s}) and α_s had considerable effect on the response of the aircraft during longitudinally accelerated flight. This

fact suggested the concept of an "equivalent disturbance"; that is, one in which the Mach number variation of the aerodynamic parameters which define C_{L_s} and α_s could be changed to suit some particular purpose, and, provided the Mach number history of C_{L_s} and α_s remained the same, the response of the airplane would remain relatively unaltered.

A close approximation to the correct solution is then obtainable by assuming C_{L_α}, C_{m_α}, $\eta_t C_{L_{\alpha_t}}$, $d\epsilon/d\alpha$, ζ, and M (where it appears in the equations of motion) constant over the Mach number range and adjusting $C_{m_o} + C_{m_{i_t}} i_t + C_{n_{\delta_e}} \delta_e$ and α_o so that the Mach number variation of C_{L_s} and α_s remains the same. For this method, it is convenient to rewrite the equations of motion in terms of the angle of attack, the angle of zero lift, and the static angle of attack, all measured from initial condition. With C_D neglected, equation (1) can then be rewritten as

$$\dot{\alpha} = \dot{\theta} - \left(\frac{1}{2} \frac{\rho a S}{m} M C_{L_\alpha} + \frac{\dot{M} + \frac{g}{a} \sin \gamma_i}{M} \right)_K \left(\alpha_{t=0} + \Delta\alpha \right) +$$

$$\left(\frac{1}{2} \frac{\rho a S}{m} M C_{L_\alpha} \right)_K \left(\alpha_{o_{t=0}} + \Delta\alpha_o \right) + \left(\frac{g}{a} \frac{\cos \gamma_i}{M} \right)_K \tag{8}$$

where, as before, the terms enclosed within parenthesis or brackets with a subscript K are constant. For steady-state conditions at t=0, equation (8) becomes

$$0 = -\left(\frac{1}{2} \frac{\rho a S}{m} M C_{L_\alpha} + \frac{g}{a} \frac{\sin \gamma_i}{M} \right)_K \alpha_{t=0} + \left(\frac{1}{2} \frac{\rho a S}{m} M C_{L_\alpha} \right)_K \alpha_{o_{t=0}} +$$

$$\left(\frac{g}{a} \frac{\cos \gamma_i}{M} \right)_K \tag{9}$$

Subtracting equation (9) from (8) gives

$$\dot{\alpha} = \dot{\theta} - \left(\frac{1}{2}\frac{\rho a S}{m} M\, C_{L_\alpha} + \frac{\dot{M} + \frac{g}{a}\sin\gamma_i}{M}\right)_K \Delta\alpha + \left(\frac{1}{2}\frac{\rho a S}{m} M\, C_{L_\alpha}\right)_K \Delta\alpha_o -$$

$$\left(\frac{\dot{M}}{M}\right)_K \alpha_{t=0} \tag{10}$$

Similarly, the pitching-moment equation becomes

$$\ddot{\theta} = \left(\frac{1}{2}\frac{\rho a^2 S\bar{c} M^2}{I_Y} C_{m_\alpha}\right)_K \left(\Delta\alpha - \Delta\alpha_s\right) - \left(\frac{1}{2}\frac{\rho a S_t l_t{}^2 M}{I_Y} n_t\, C_{L_{\alpha_t}}\right)_K \Bigg[(\zeta)_K\, \dot{\theta} +$$

$$\left(\frac{d\epsilon}{d\alpha}\right)_K \dot{\alpha}\Bigg] \tag{11}$$

Combining equations (10) and (11) as before, the resulting differential equation is

$$\Delta\ddot{\alpha} + b'\Delta\dot{\alpha} + k'\Delta\alpha = f' \tag{12}$$

where

$$b' = \left[\frac{1}{2}\frac{\rho a S}{m} M\, C_{L_\alpha} + \frac{\dot{M} + \frac{g}{a}\sin\gamma_i}{M} + \frac{1}{2}\frac{\rho a S_t l_t{}^2 M}{I_Y} n_t\, C_{L_{\alpha_t}} \left(\zeta + \frac{d\epsilon}{d\alpha}\right)\right]_K$$

$$k' = \Bigg[-\frac{1}{2}\frac{\rho a^2 S\bar{c}}{I_Y} M^2\, C_{m_\alpha} + \frac{1}{2}\frac{\rho a S_t l_t{}^2}{I_Y} M\, n_t\, C_{L_{\alpha_t}}\, \zeta \Bigg(\frac{1}{2}\frac{\rho a S}{m} M\, C_{L_\alpha} +$$

$$\frac{\dot{M} + \frac{g}{a}\sin\gamma_i}{M}\Bigg)\Bigg]_K$$

$$f' = \left(-\frac{1}{2}\frac{\rho a^2 S\bar{c}}{I_Y} M^2\, C_{m_\alpha}\right)_K \Delta\alpha_s + \left(\frac{1}{2}\frac{\rho a S}{m} M\, C_{L_\alpha}\right)_K \Delta\dot{\alpha}_o +$$

$$\left(\frac{1}{2}\,\frac{\rho a S_t l_t^2 M}{I_Y} n_t\, C_{L_{\alpha_t}}\, \zeta\, \frac{1}{2}\,\frac{\rho a S}{m}\, M\, C_{L_\alpha}\right)_K \Delta\alpha_o$$

the negligible constant term

$$\left(\frac{1}{2}\,\frac{\rho a S_t l_t^2}{I_Y}\, n_t\, C_{L_{\alpha_t}}\, \zeta\, \dot{M}\, \alpha_{t=0}\right)_K$$

being omitted from f'. Equation (12) is now of the form where the principle of superposition applies and Duhamel's integral theorem may be used to calculate $\Delta\alpha$ due to the irregular variation of the disturbance f'. A semigraphical application of this theorem which was applied in reference 1 to the calculation of the motion of an airplane under the influence of irregular disturbances and more recently in reference 2 was used for the present computations. This method reduces essentially to the solution of equation (12) for a unit step-forcing function f'(1) and the combination of this response with the variable f' by means of Duhamel's integral through use of a simple graphical procedure.

Results and discussion.- The assumed equivalent-disturbance parameters, along with the original variation of the parameters with Mach number for the same examples as shown in figure 7 are presented in figure 8. The values of C_{L_α}, C_{m_α}, $n_t\, C_{L_{\alpha_t}}$, ζ, and $d\epsilon/d\alpha$ represent average values over the range from the initial Mach number to the Mach number for maximum change in A_{n_s}; it was found that these magnitudes give good results. The Mach number at the maximum change in A_{n_s} was used in computing the coefficients b', k', and f'.

Figure 9 illustrates the graphical integration procedure for one of the examples at a specified instant of time, and is discussed in detail in the appendix.

Figure 10 shows the good agreement between the computations by this method and the differential-analyzer answers for the same two longitudinal accelerations used in the modified step-by-step method comparison. The method is relatively rapid, the first case requiring approximately two computer days and each succeeding case about three-quarters of a computer day. It should be noted that if the effect of $\dot{M}$ upon b' and k' is small, the response to a step input f'(1) need be computed only once, a very important time-saving factor if a number of longitudinal accelerations are to be investigated.

An evident inaccuracy arises from the use of a constant Mach number in the simplified equations of motion in place of the true Mach number variation over the range being investigated. It is believed, therefore, that this method should be applied only to a balance change, the Mach number range of which is small.

CONCLUSIONS

As a result of an investigation to determine the effect on the motion experienced by a hypothetical, small, straight-wing aircraft when accelerated at various rates through an assumed controls-fixed pitch-down balance change in the transonic range, the following conclusions may be made:

1. The maximum change in normal acceleration increases with increasing longitudinal acceleration up to a certain magnitude of longitudinal acceleration, after which it decreases with further increases in longitudinal acceleration.

2. The Mach number variation of the angle of attack for static balance determines to a great extent the degree of the effect of longitudinal acceleration on the normal acceleration.

3. Changes in altitude, initial flight-path angle, moment of inertia and a factor representative of the Mach number range of the balance change (defined herein as the Mach number width) have little effect on the magnitude of the peak of the ratio of the maximum change in dynamic to static-balanced normal acceleration, but an increase in moment of inertia and altitude and a decrease in Mach number width decreases the magnitude of the average longitudinal acceleration at which this peak occurs.

4. The two approximate analytical methods for solving the equations of motion which were developed give good results for the assumed balance change. The modified step-by-step method appears to be applicable to all problems of this type. However, the accuracy of the equivalent-disturbance method has not been adequately investigated so its use should be limited to cases similar to the one investigated.

5. The methods presented herein may be used to study the effects of longitudinal acceleration on the results obtained from rocket models flown to determine the static and dynamic stability characteristics and as an aid in planning flight programs to avoid the effects of longitudinal acceleration on these characteristics.

It is difficult to generalize on the basis of the results of this brief investigation, but it is believed that the above noted trends indicated should apply to any similar balance change.

Ames Aeronautical Laboratory,
National Advisory Committee for Aeronautics,
Moffett Field, Calif.

APPENDIX

CALCULATION OF THE INCREMENTAL ANGLE OF ATTACK $\Delta\alpha$ FOR ANY VARIATION OF THE FORCING FUNCTION f'

The solutions of equation (12) for a unit step function $f'(1)$ can take any one of three forms, as explained in the section on the modified step-by-step method, but only the solution for $k' > (b'/2)^2$ will be presented in the following equation:

$$\frac{\Delta\alpha k'}{f'(1)} = 1 + e^{-(b'/2)t} \left\{ \frac{\Delta\dot{\alpha}_{t=0}\, k' - (b'/2)}{\sqrt{k' - (b'/2)^2}} \sin\left[\sqrt{k' - (b'/2)^2}\; t\right] - \cos\left[\sqrt{k' - (b'/2)^2}\; t\right] \right\}$$

The graphical method for combining the response of a unit disturbance with the variable forcing function f' can best be understood by following a sample computation. The work sheet for an example is shown in figure 9, and the procedure is as follows:

1. Plot $\Delta\alpha k'/f'(1)$ as a function of time to some convenient scale.

2. Plot f' as a function of time using the same time scale.

3. Select a time t_o at which the $\Delta\alpha$ due to f' is desired. Project the point on the f' curve corresponding to this time horizontally until it intersects the 45° line. This line is then deflected vertically until it intersects the horizontal projection of $\Delta\alpha k'/f'(1)$ at $t=0$. This establishes the point labeled (1).

4. The ordinate of the f' curve at some time less than t_o by the amount Δt is next projected as before until it intersects the horizontal projection of the $\Delta\alpha k'/f'(1)$ at Δt. The point (2) is obtained in this manner.

5. Other points are similarly obtained to complete the closed curve for the time t_o. Note that the addition of t on the f' curve and t on the $\Delta\alpha k'/f'(1)$ always equals t_o. The area encompassed by the curve is proportional to $\Delta\alpha$ at time t_o.

6. The area is found by integrating in the direction (0), (1), (2), etc. If a counterclockwise path is followed in enclosing the area, the value is positive regardless of the quadrants involved and vice versa for clockwise integration.

7. Other curves are drawn for different times. The final step is to correct the areas into the $\Delta\alpha$ associated with the function f' by multiplying the areas by the appropriate scale factors of $\Delta\alpha k'/f'(1)$ and f' and dividing by k'. The lift coefficient is equal to $C_{L_{\alpha_{assumed}}}$ $(\alpha_{t=0} + \Delta\alpha - \alpha_{o_{assumed}})$. The correct angle of attack can be obtained from the formula $\alpha = \dfrac{C_L}{C_{L_{\alpha_{true}}}} + \alpha_{o_{true}}$ and the angle of pitch from equation (1).

REFERENCES

1. Jones, Robert T.: Calculation of the Motion of an Airplane under the Influence of Irregular Disturbances. Jour. Aero. Sci., vol. 3, no. 12, Oct. 1936, pp. 419–425.

2. Pearson, Henry A.: Derivation of Charts for Determining the Horizontal Tail Load Variation with Any Elevator Motion. NACA Rep. 759, 1943.

TABLE I.– COMPUTATIONS OF NORMAL ACCELERATION BY MODIFIED STEP-BY-STEP METHOD
[Characteristics (a) of figure 1, average longitudinal acceleration of 1.37]

Column	(1)	(2)	(3)	(4)	(5)	(6)	(7)	(8)	(9)	(10)	(11)	(12)	(13)	(14)	(15)	(16)	(17)	(18)	(19)	(20)	(21)
row, r	M	b	k	f_o	$\frac{df_o}{dM}$	$\frac{(2)}{2}$	(3) − (6)²	$\sqrt{(7)}$	57.3 × $\frac{\Delta M}{\dot{M}}$ × (8)	cos (9)	sin (9)	$\frac{-\Delta M}{\dot{M}}$ × (6)	(12)	(10) × (13)	(11) × (13)	$\dot{M}$ × (5)	$\frac{(16)}{(3)}$	(2) × (17)	$\frac{(4)_{r-1} - (18)}{(3)}$	$\frac{\Delta M}{\dot{M}}$ × (17)	(19) + (20)
1	0.90			0.426																	
2		1.164	9.80		-4.30	0.582	9.46	3.08	77.51	0.216	0.976	-0.256	0.774	0.1675	0.7560	-0.1957	-0.0200	-0.0233	0.0458	-0.0088	0.0370
3	.92			.340																	
4		1.156	11.00		-2.65	.578	10.67	3.27	82.30	.134	.991	-.254	.776	.1039	.7686	-.1206	-.0110	-.0127	.0321	-.0048	.0273
5	.94			.287																	
6		1.129	12.00		-1.75	.564	11.68	3.42	86.13	.067	.998	-.248	.780	.0527	.7784	-.0796	-.0066	-.0075	.0245	-.0029	.0216
7	.96			.252																	
8		1.082	12.95		-.75	.541	12.66	3.56	89.65	.006	1.000	-.238	.788	.0048	.7883	-.0341	-.0026	-.0028	.0197	-.0011	.0186
9	.98			.237																	
10		1.023	13.80		1.05	.511	13.54	3.68	92.72	-.047	.999	-.225	.799	-.0379	.7977	.0478	.0035	.0036	.0169	.0015	.0184
11	1.00			.258																	
12		1.002	14.65		3.40	.501	14.40	3.79	95.62	-.098	.995	-.220	.802	-.0786	.7985	.1547	.0106	.0106	.0169	.0047	.0216
13	1.02			.326																	
14		1.054	16.30		2.15	.527	16.02	4.00	100.9	-.189	.982	-.232	.793	-.1496	.7790	.0978	.0060	.0063	.0196	.0026	.0222
15	1.04			.369																	
16		1.169	19.30		0	.584	18.96	4.35	109.7	-.337	.941	-.257	.773	-.2610	.7281	0	0	0	.0191	0	.0191
17	1.06			.369																	
18		1.300	22.95		-.60	.650	22.53	4.75	119.6	-.494	.869	-.286	.751	-.3713	.6533	-.0273	-.0012	-.0016	.0161	-.0005	.0156
19	1.08			.357																	
20		1.408	27.05		-1.40	.704	26.55	5.15	129.9	-.641	.768	-.310	.734	-.4703	.5633	-.0637	-.0024	-.0034	.0133	-.0011	.0122
21	1.10			.389																	

Column		(22)	(23)	(24)	(25)	(26)	(27)	(28)	(29)	(30)	(31)	(32)	(33)	(34)	(35)	(36)	(37)	(38)	(39)	(40)	(41)
row, r	M	α = $(30)_{r-1}$	$\dot{\alpha}$ = $(37)_{r-1}$	$(22)_{r-1}$ − (19)	(24) × (6)	$(23)_{r-1}$ − (17) + (25)	$\frac{(26)}{(8)}$	(14) × (24)	(15) × (27)	(21) + (28) + (29)	(26) − (25)	(6) × (27)	(8) × (24)	(32) + (33)	(14) × (31)	−(15) × (34)	(17) + (35) + (36)	57.3 × (22)	(38) − α_o	C_L = C_{L_α} × (39)	Δn = $\frac{(40)}{C_{L_{trim}}}$
1	0.90	0.0459	-0.0023															2.63	3.63	0.363	1.00
2				0.0001	0.0001	0.0178	0.0058	0	0.0044	0.0414	0.0177	0.0034	0.0003	0.0037	0.0030	-0.0028	-0.0198				
3	.92	.0414	-.0198															2.37	3.00	.295	.85
4				.0093	.0054	-.0034	-.0010	.0010	-.0008	.0275	-.0088	-.0006	.0304	.0298	-.0009	-.0229	-.0348				
5	.94	.0275	-.0348															1.58	1.86	.175	.53
6				.0030	.0017	-.0865	-.0078	.0002	-.0061	.0157	-.0882	-.0044	.0103	.0059	-.0015	-.0046	-.0127				
7	.96	.0157	-.0127															.90	.85	.076	.24
8				-.0040	-.0022	-.0123	-.0035	0	-.0028	.0158	-.0101	-.0019	-.0142	-.0161	0	.0127	.0101				
9	.98	.0158	.0101															.91	.56	.046	.15
10				-.0011	-.0006	.0060	.0016	0	.0013	.0197	.0066	.0008	-.0040	-.0032	-.0003	.0086	.0059				
11	1.00	.0197	.0059															4.13	.63	.047	.16
12				.0028	.0014	-.0033	-.0009	-.0002	-.0007	.0207	-.0047	-.0004	.0106	.0102	.0004	-.0081	.0029				
13	1.02	.0207	.0029															1.19	.87	.068	.24
14				.0011	.0006	-.0025	-.0006	-.0002	-.0005	.0216	-.0031	-.0003	.0044	.0041	.0005	-.0032	.0033				
15	1.04	.0216	.0033															1.24	1.28	.112	.41
16				.0025	.0015	.0048	.0011	-.0007	.0008	.0193	.0033	.0006	.0109	.0115	-.0009	-.0084	-.0093				
17	1.06	.0193	-.0093															1.11	1.48	.147	.56
18				.0032	.0021	-.0060	-.0013	-.0012	-.0009	.0136	-.0081	-.0009	.0152	.0144	.0030	-.0094	-.0076				
19	1.08	.0136	-.0076															.78	1.47	.160	.64
20				.0003	.0002	-.0050	-.0010	-.0001	-.0006	.0115	-.0052	-.0007	.0015	.0008	-.0025	-.0005	-.0054				
21	1.10	.0115	-.0054															.66	1.64	.189	.78

NACA

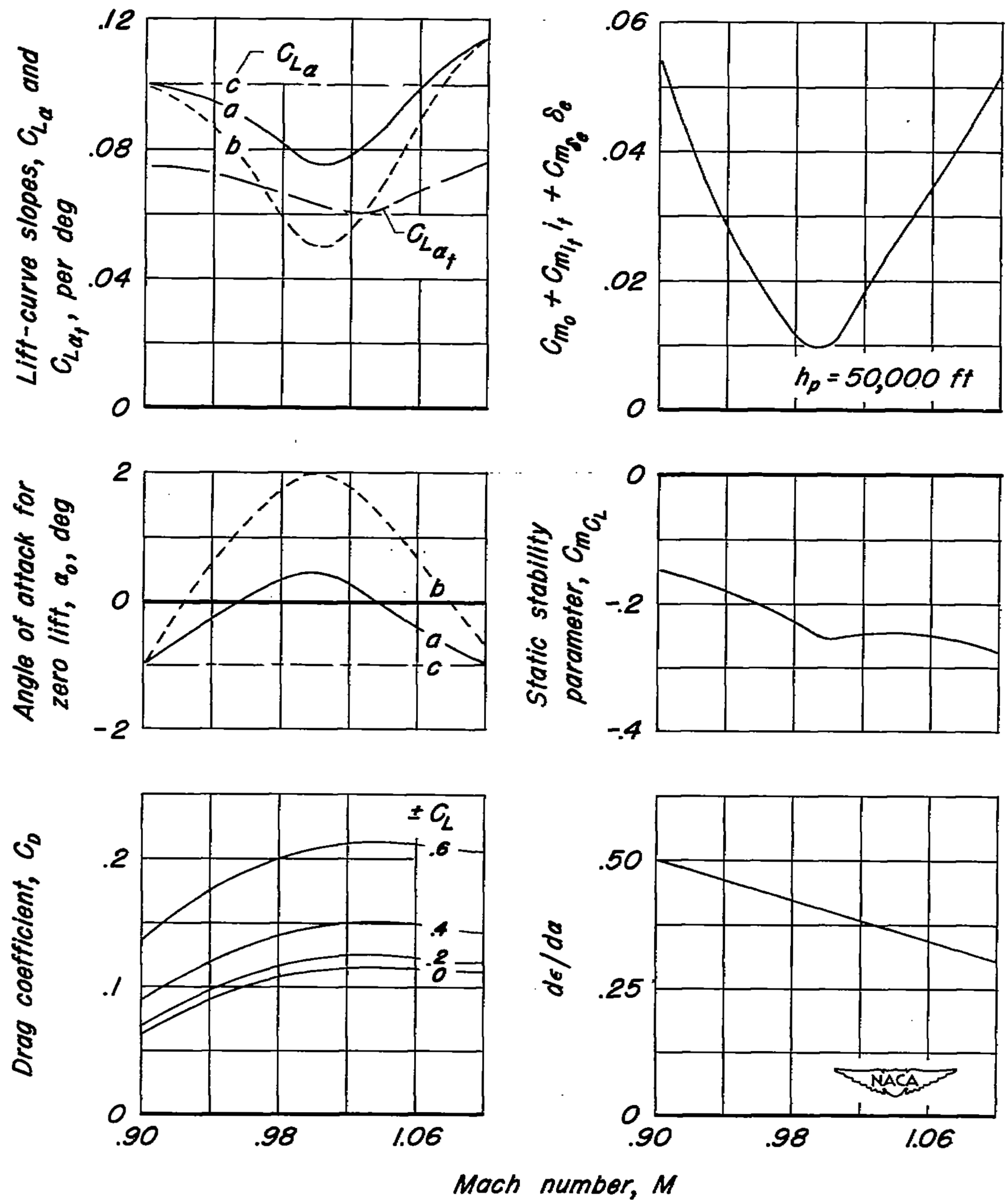

Figure 1.- Assumed variation of aerodynamic parameters with Mach number for the hypothetical airplane.

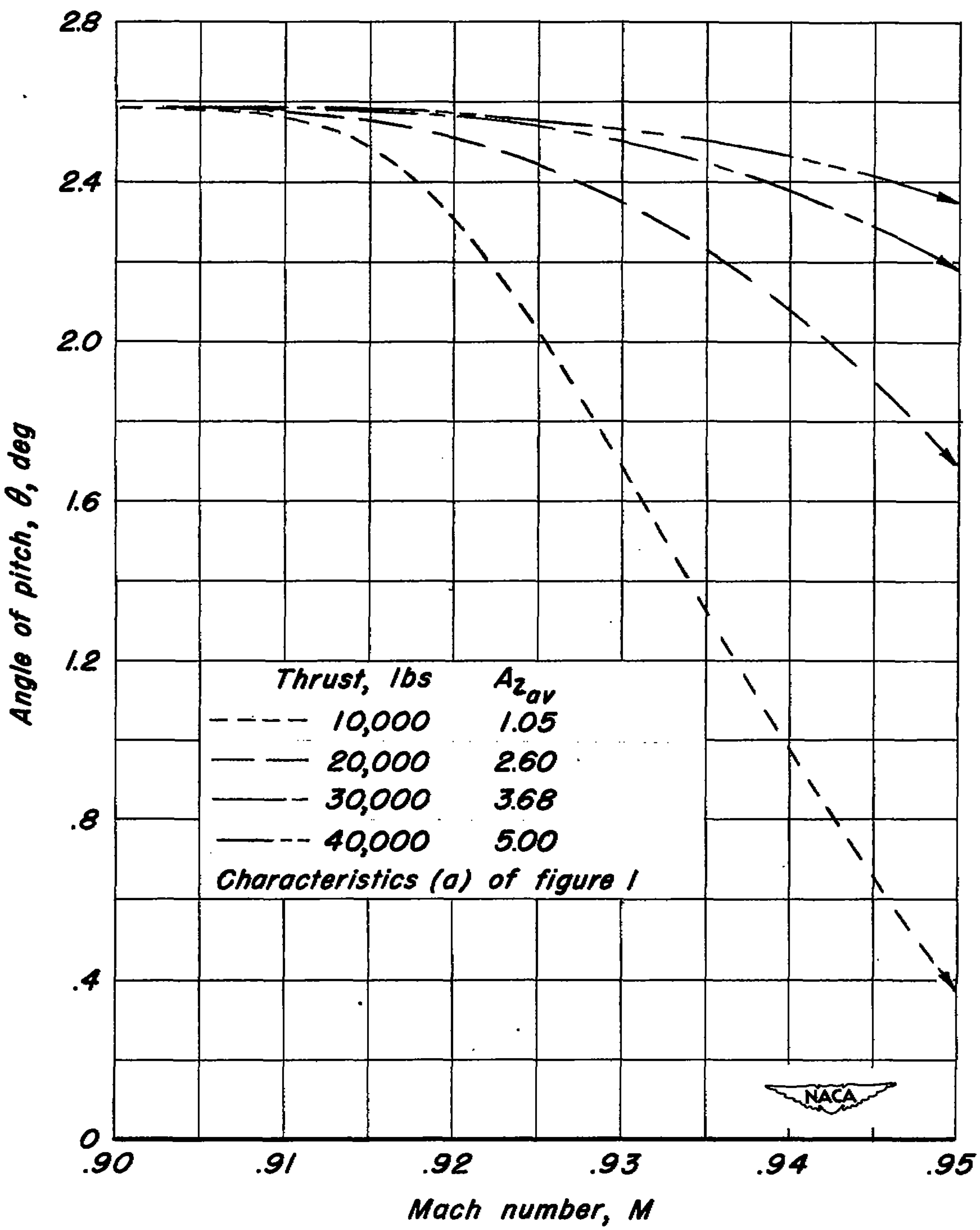

Figure 2.- Effect of longitudinal acceleration on the initial response in pitch.

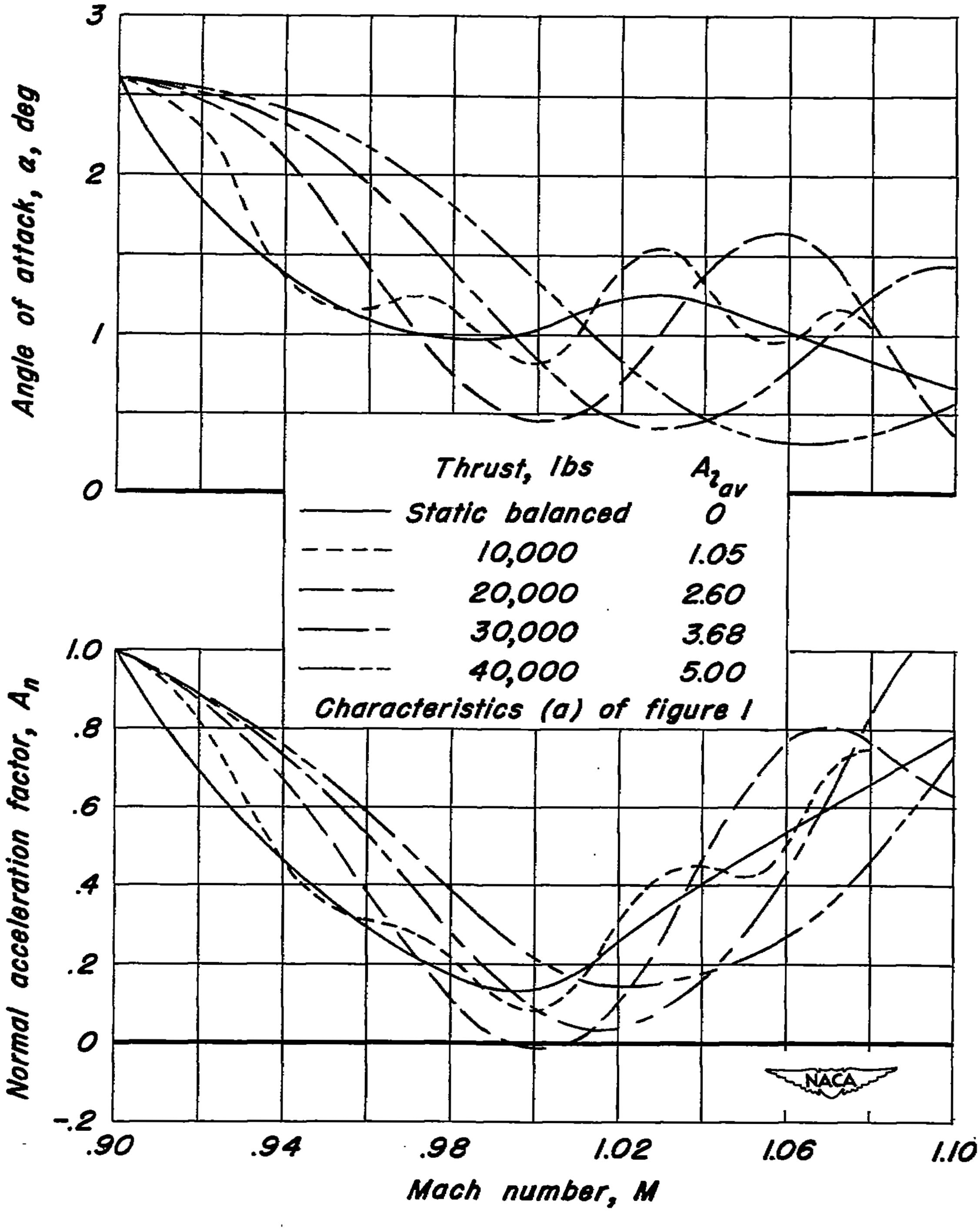

Figure 3.– Effect of longitudinal acceleration on the angle of attack and normal acceleration factor.

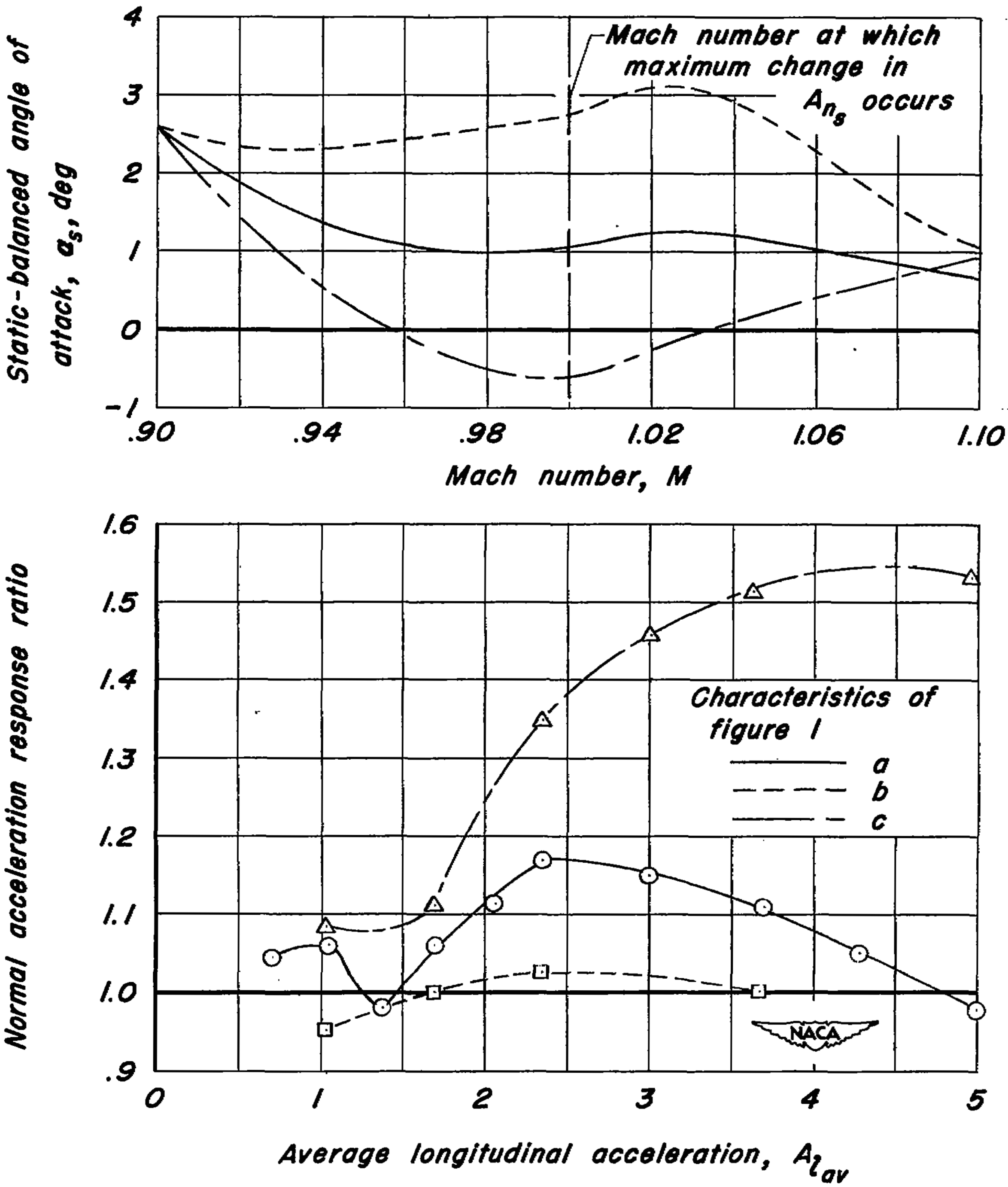

Figure 4.- Effect of longitudinal acceleration on the normal acceleration response ratio for three variations of α_s with Mach number but identical variation of A_{n_s} with Mach number.

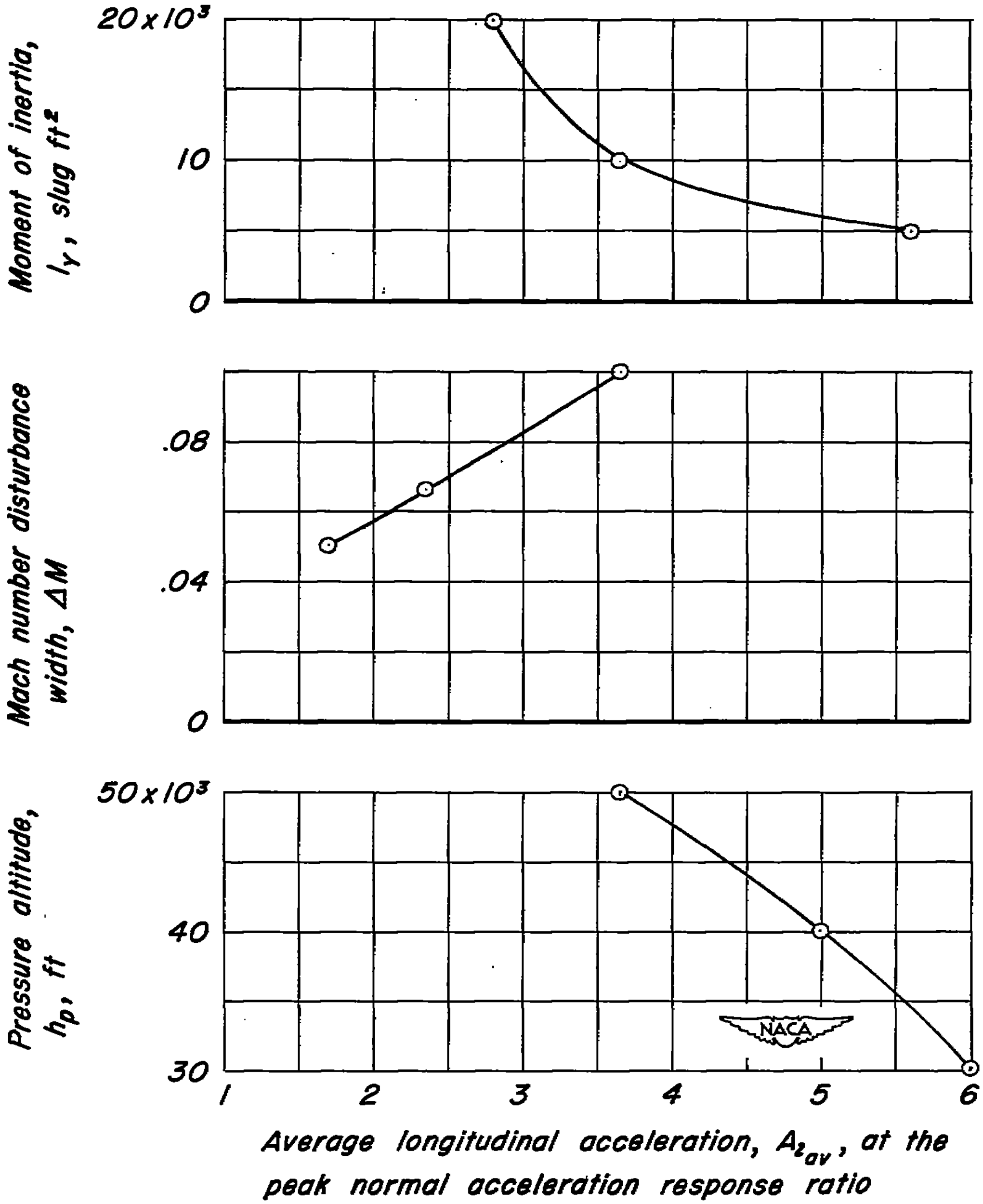

Figure 5.- Effect of changes in moment of inertia, Mach number disturbance width, and pressure altitude on the average longitudinal acceleration at which the peak normal acceleration response ratio occurs.

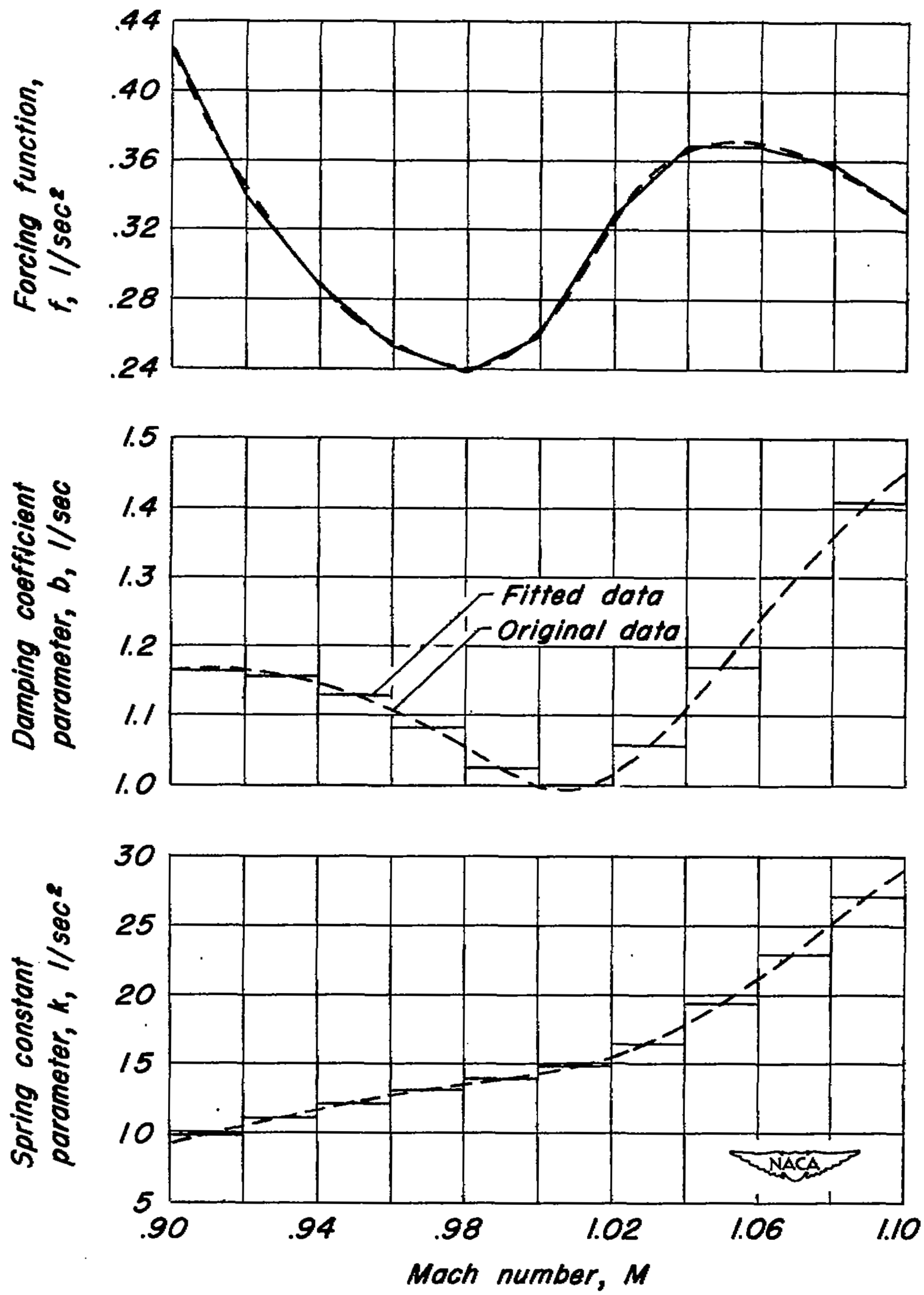

Figure 6.– Example of curve-fitting method. Characteristics (a) of figure 1, average longitudinal acceleration of 1.37.

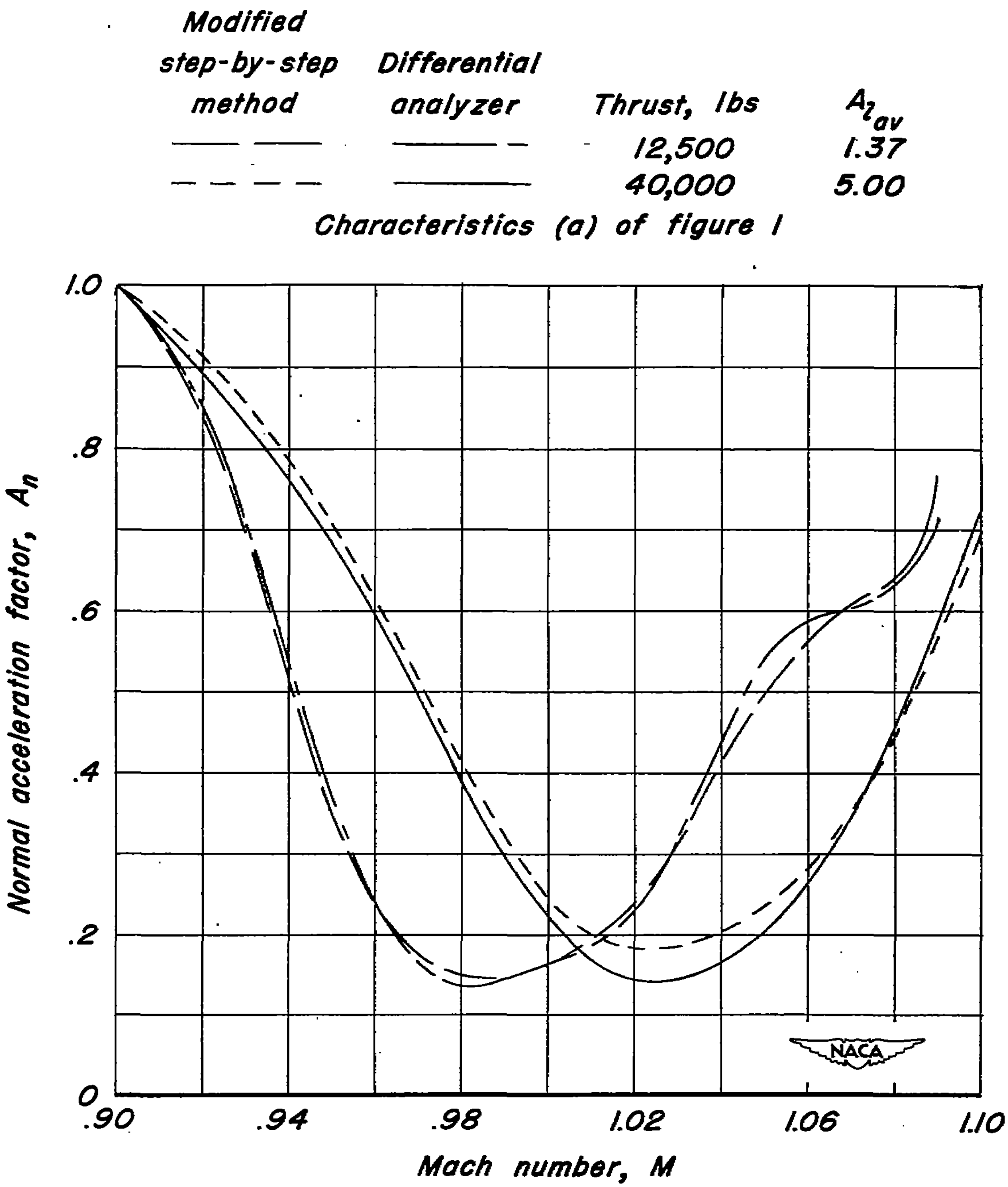

Figure 7.- Comparison of normal acceleration factor computed by the modified step-by-step method and by the differential analyzer.

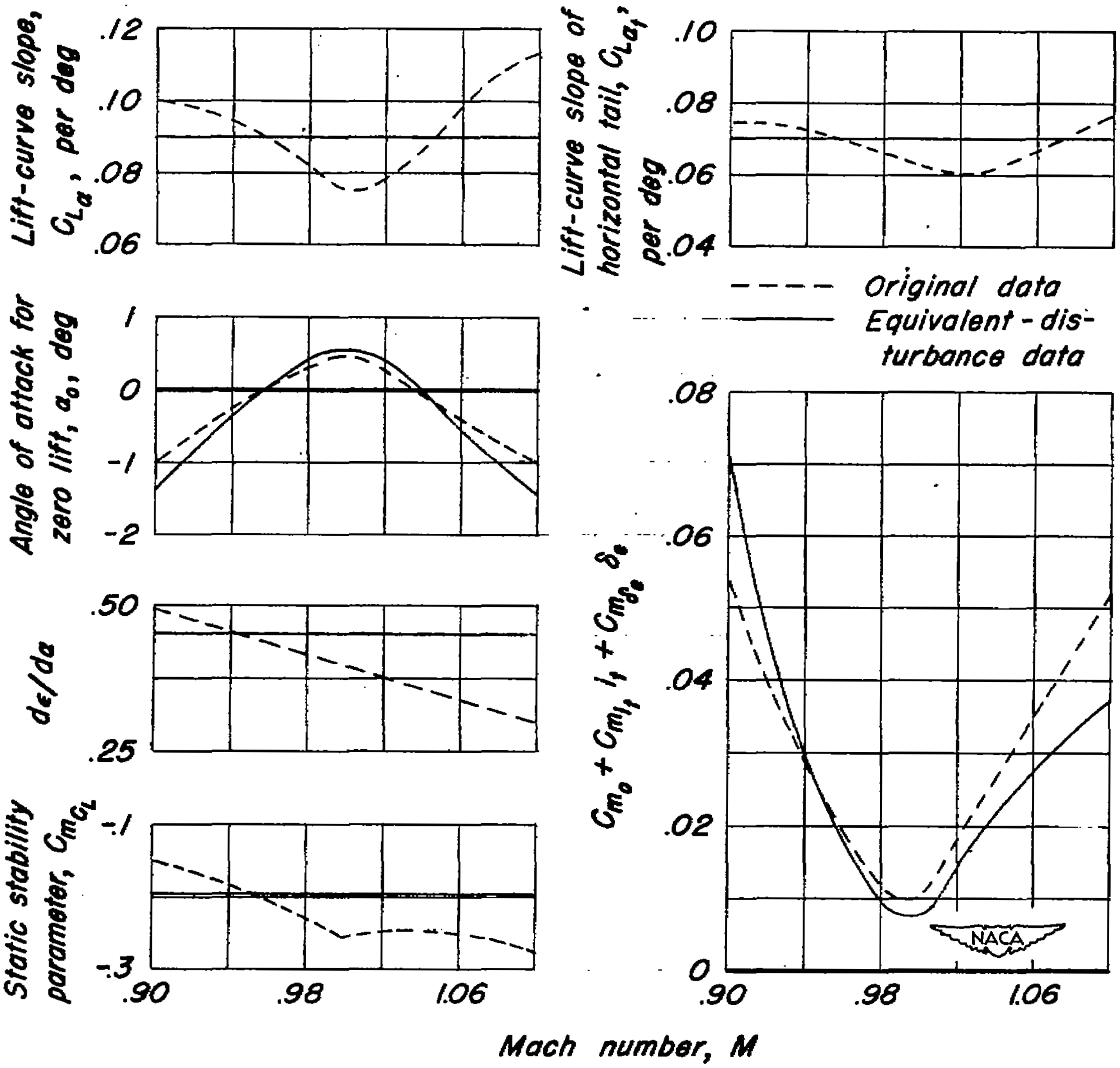

Figure 8.- Mach number histories of original and equivalent-disturbance method data. Average longitudinal acceleration of 1.37.

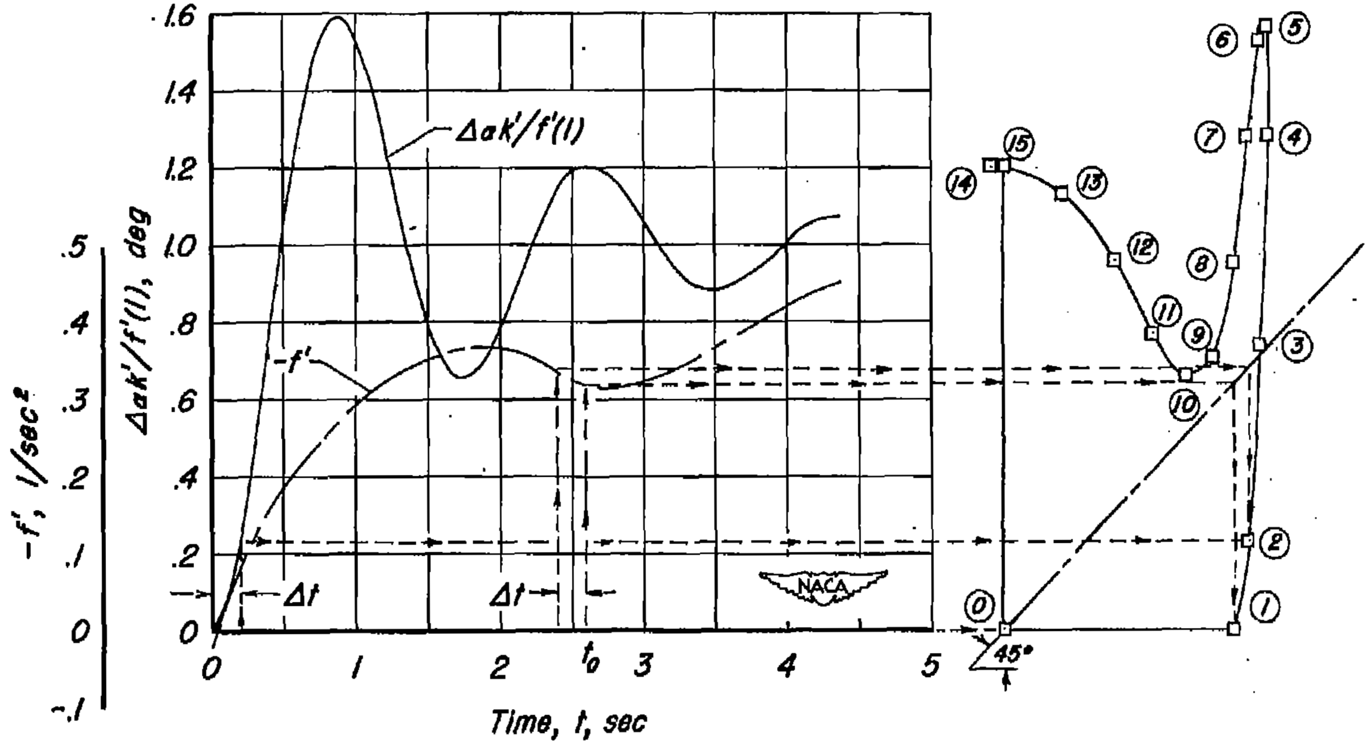

Figure 9.- Example of the graphical procedure for the determination of the incremental angle of attack $\Delta\alpha$. Average longitudinal acceleration of 1.37.

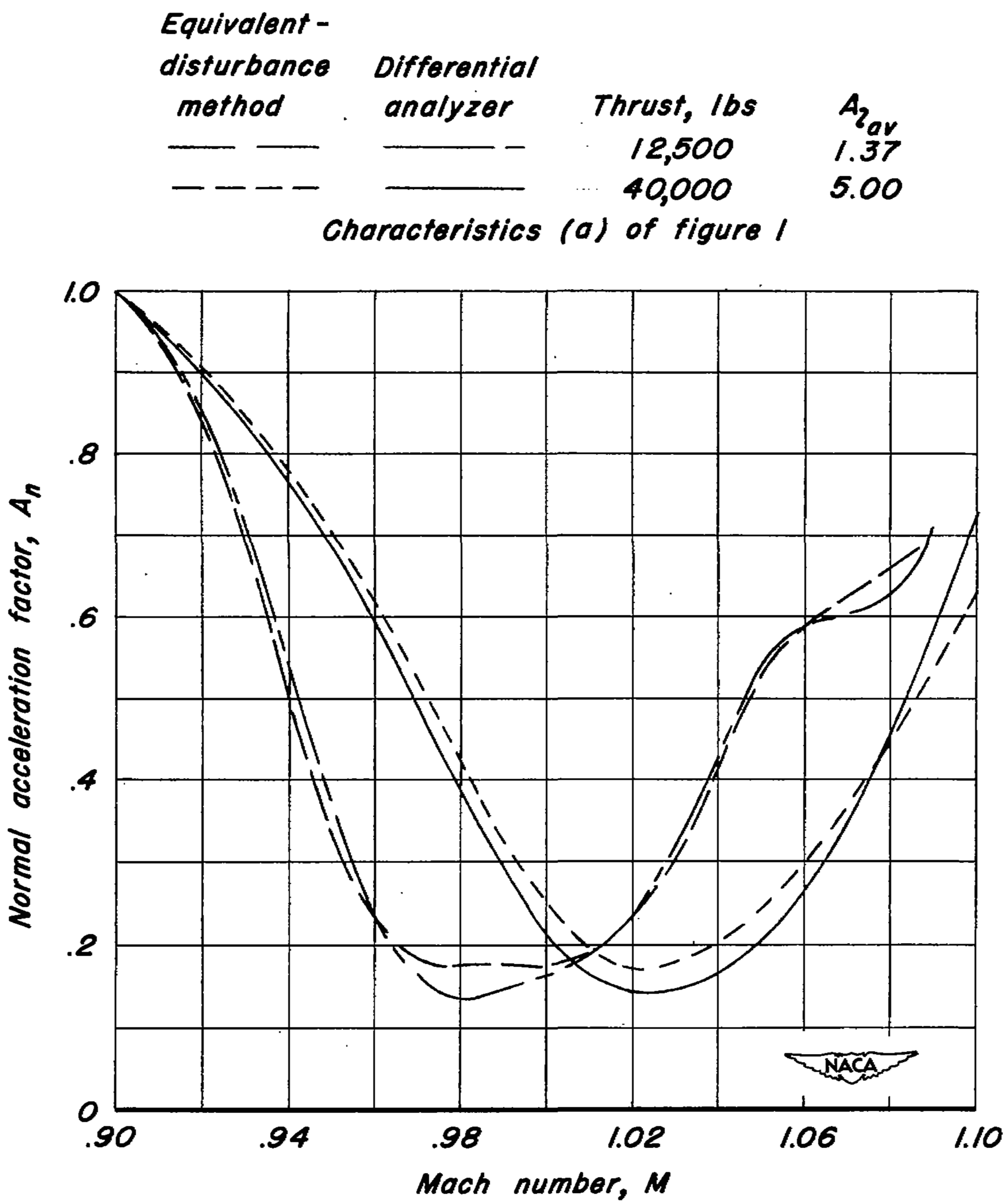

Figure 10.– Comparison of normal acceleration factor computed by the equivalent-disturbance method and by the differential analyzer.